



**GASTROINTESTINAL, HEPATOBILIARY, AND PANCREATIC PATHOLOGY**

# Nicotine Promotes Cholangiocarcinoma Growth in Xenograft Mice



Allyson K. Martínez,<sup>\*</sup> Kendal Jensen,<sup>†</sup> Chad Hall,<sup>‡</sup> April O'Brien,<sup>\*</sup> Laurent Ehrlich,<sup>\*</sup> Tori White,<sup>\*</sup> Fanyin Meng,<sup>\*§¶</sup> Tianhao Zhou,<sup>\*</sup> John Greene, Jr,<sup>||</sup> Francesca Bernuzzi,<sup>\*\*††</sup> Pietro Invernizzi,<sup>\*\*††</sup> David E. Dostal,<sup>†§</sup> Terry Lairmore,<sup>‡</sup> Gianfranco Alpini,<sup>\*†§¶</sup> and Shannon S. Glaser<sup>\*§¶</sup>

From the Departments of Internal Medicine,<sup>\*</sup> Medical Physiology,<sup>†</sup> and Surgery,<sup>‡</sup> Texas A&M Health Science Center, College of Medicine, Temple, Texas; Central Texas Veterans Health Care System,<sup>§</sup> Temple, Texas; the Department of Pathology<sup>||</sup> and the Digestive Disease Research Center,<sup>¶</sup> Baylor Scott & White Health, Temple, Texas; the Program for Autoimmune Liver Diseases,<sup>\*\*</sup> International Center for Digestive Health, Department of Medicine and Surgery, University of Milan-Bicocca, Milan, Italy; and the Humanitas Clinical and Research Center,<sup>††</sup> Rozzano, Milan, Italy

Accepted for publication  
January 17, 2017.

Address correspondence to  
Shannon S. Glaser, Ph.D.,  
Texas A&M Health Science  
Center, 1901 S. First St., VA  
Bldg. 205, Temple,  
TX 76504. E-mail: [sglaser@  
medicine.tamhsc.edu](mailto:sglaser@medicine.tamhsc.edu).

Nicotine, the main addictive substance in tobacco, is known to play a role in the development and/or progression of a number of malignant tumors. However, nicotine's involvement in the pathogenesis of cholangiocarcinoma is controversial. Therefore, we studied the effects of nicotine on the growth of cholangiocarcinoma cells *in vitro* and the progression of cholangiocarcinoma in a mouse xenograft model. The predominant subunit responsible for nicotine-mediated proliferation in normal and cancer cells, the  $\alpha 7$  nicotinic acetylcholine receptor ( $\alpha 7$ -nAChR), was more highly expressed in human cholangiocarcinoma cell lines compared with normal human cholangiocytes. Nicotine also stimulated the proliferation of cholangiocarcinoma cell lines and promoted  $\alpha 7$ -nAChR-dependent activation of proliferation and phosphorylation of extracellular-regulated kinase in Mz-ChA-1 cells. In addition, nicotine and PNU282987 ( $\alpha 7$ -nAChR agonist) accelerated the growth of the cholangiocarcinoma tumors in our xenograft mouse model and increased fibrosis, proliferation of the tumor cells, and phosphorylation of extracellular-regulated kinase activation. Finally,  $\alpha 7$ -nAChR was expressed at significantly higher levels in human cholangiocarcinoma compared with normal human control liver samples. Taken together, results of this study suggest that nicotine acts through  $\alpha 7$ -nAChR and plays a novel role in the pathogenesis of cholangiocarcinoma. Furthermore, nicotine may act as a mitogen in cholestatic liver disease processes, thereby facilitating malignant transformation. (*Am J Pathol* 2017, 187: 1093–1105; <http://dx.doi.org/10.1016/j.ajpath.2017.01.011>)

Tobacco is the leading cause of preventable death worldwide, contributing to the deaths of 6 million people per year.<sup>1</sup> Tobacco has a known role in the development of a number of malignant tumors, including lung, esophageal, and pancreatic cancers.<sup>2–4</sup> However, there is conflicting evidence as to whether tobacco plays a role in the development and/or progression of cholangiocarcinoma (CCA).<sup>5–9</sup>

Nicotine is the main addictive substance in tobacco and has profound effects on mood, appetite, and task performance.<sup>10</sup> Nicotine is a tertiary amine that consists of a pyridine and pyrrolidine ring, which is rapidly absorbed through epithelial barriers before entering the bloodstream.<sup>11–13</sup> After entering the bloodstream, nicotine circulates throughout the body, binding to cells that express nicotinic acetylcholine receptors

(nAChRs), including cholangiocytes.<sup>11–13</sup> Out of the 17 different nAChRs subunits identified,  $\alpha 7$ -nAChR is the predominant subunit responsible for nicotine-mediated proliferation in normal and cancer cells.<sup>14,15</sup> Stimulation of  $\alpha 7$ -nAChR triggers an influx of calcium that activates downstream signaling mechanisms, including

Supported by resources at the Central Texas Veterans Health Care System and in part by VA Merit Awards 5I01BX002192 (S.S.G.) and 5I01BX000574 (G.A.) from the US Department of Veterans Affairs Biomedical Laboratory Research and Development Service.

A.K.M. and K.J. contributed equally as first authors.

Disclosures: None declared.

The views expressed in this article are those of the authors and do not necessarily represent the views of the US Department of Veterans Affairs.

phosphorylation of extracellular-regulated kinase (p-ERK), which promotes cell proliferation.<sup>16</sup>

CCA is an aggressive tumor that arises from the epithelial cells that line the biliary tree.<sup>17,18</sup> CCA comprises approximately 10% to 15% of total liver tumors and increases in incidence every year.<sup>17</sup> The increase in incidence observed with CCA can be partially attributed to the fact that preexisting liver disease, including primary biliary cirrhosis (PBC), primary sclerosing cholangitis (PSC), and graft-versus-host disease, is a risk factor for the development of CCA.<sup>19</sup> Because of a lack in the understanding of the molecular mechanisms that regulate CCA growth, surgical resection is generally the only viable treatment option; however, most tumors are inoperable.<sup>18,20</sup> Therefore, gaining a full understanding of the risk factors and determining the molecular mechanisms that regulate CCA growth are essential for the development of more treatment options for patients with CCA. Our aim was to evaluate the effects of nicotine on CCA proliferation and in CCA development and growth in a xenograft mouse model.

## Materials and Methods

### Cell Culture

The normal human intrahepatic biliary epithelial cell (HIBEpiC) line was obtained from ScienCell Research Laboratories (Carlsbad, CA) and cultured according to the vendor's instructions. The extrahepatic cell line Mz-ChA-1 was a gift from Dr. J. Gregory Fitz (UT Southwestern, Dallas, TX) and cultured as previously described.<sup>21</sup> The intrahepatic cell lines HuCC-T1 and CCLP1 were a gift from Dr. Anthony J. Demetris (University of Pittsburgh, Pittsburgh, PA) and cultured as previously described.<sup>22,23</sup>

### Assessment of $\alpha 7$ -nAChR Expression in Normal Human Cholangiocytes and CCA Cell Lines

#### Immunofluorescence

Cells were seeded at 10,000 cells per well into six-well plates that contained sterile coverslips and allowed to adhere overnight. Cells were washed once in cold phosphate-buffered saline (PBS), fixed with 4% paraformaldehyde in PBS, permeabilized in PBS that contained 0.2% Triton X-100, and blocked with 5% bovine serum albumin for 1 hour at room temperature.  $\alpha 7$ -nAChR antibody (1:100, ab10096) (Abcam, Cambridge, MA) was added to the coverslips, and incubated at 4°C overnight (24 hours). Cells were washed 3 × 10 minutes in PBS with 0.2% Triton X-100, and a Cy2 anti-rabbit secondary antibody was used (1:50) (Jackson ImmunoResearch Laboratories, West Grove, PA). Cells were washed again and mounted onto microscope slides with ProLong Gold Antifade that contained DAPI as a counterstain (Molecular Probes, Eugene, OR). Negative controls were processed similarly with the omission of the  $\alpha 7$ -nAChR

antibody. Sections were visualized using an Olympus IX-71 inverted confocal microscope.

### FACS Analysis

The expression of  $\alpha 7$ -nAChR in normal human cholangiocytes (HIBEpiC) and the CCA cell lines was evaluated with a BD Accuri C6 Flow Cytometer (BD Biosciences, San Jose, CA). Briefly, 10,000 cells were used to determine the protein expression levels. The cells were fixed in 4% paraformaldehyde and then incubated with the selected primary antibody followed by incubation with Molecular Probes secondary antibody (Alexa Fluor 488 or 350), corresponding to the primary antibody species. The labeled cells were evaluated and the fluorescence-activated cell sorting (FACS) data were analyzed with C6Flow software version 1.0.264.21 (BD Biosciences).

### Assessment of Nicotine's Effect on Proliferation by MTS Assay

Normal human cholangiocytes (HIBEpiC) and the CCA cell lines were treated at 37°C for 48 hours with 0.2% bovine serum albumin (basal) or nicotine (5, 10, 15, and 20  $\mu\text{mol/L}$ ) before evaluation of cell proliferation with the CellTiter96 Cell Proliferation Assay (Promega, Madison, WI). Previous studies have used similar dosage ranges for *in vitro* studies with nicotine.<sup>14,24–26</sup> Briefly, cells were seeded (7000 cells per well) onto 96-well plates in complete medium and allowed to adhere overnight at 37°C. Cells were then serum starved in medium that contained 0.5% fetal bovine serum for 24 hours, washed twice with 1 × PBS; eight replicates were subsequently treated with dimethyl sulfoxide (vehicle) or different agents. Cells were incubated for 48 hours with the respective treatments, at which time 10  $\mu\text{L}$  of Cell Titer 96 was added to each well. Absorbance at 490 nm was determined with a microplate reader (Spectra Max 3400, Molecular Devices, Sunnyvale, CA). Absorbance is directly correlated to the number of viable cells.<sup>27</sup>

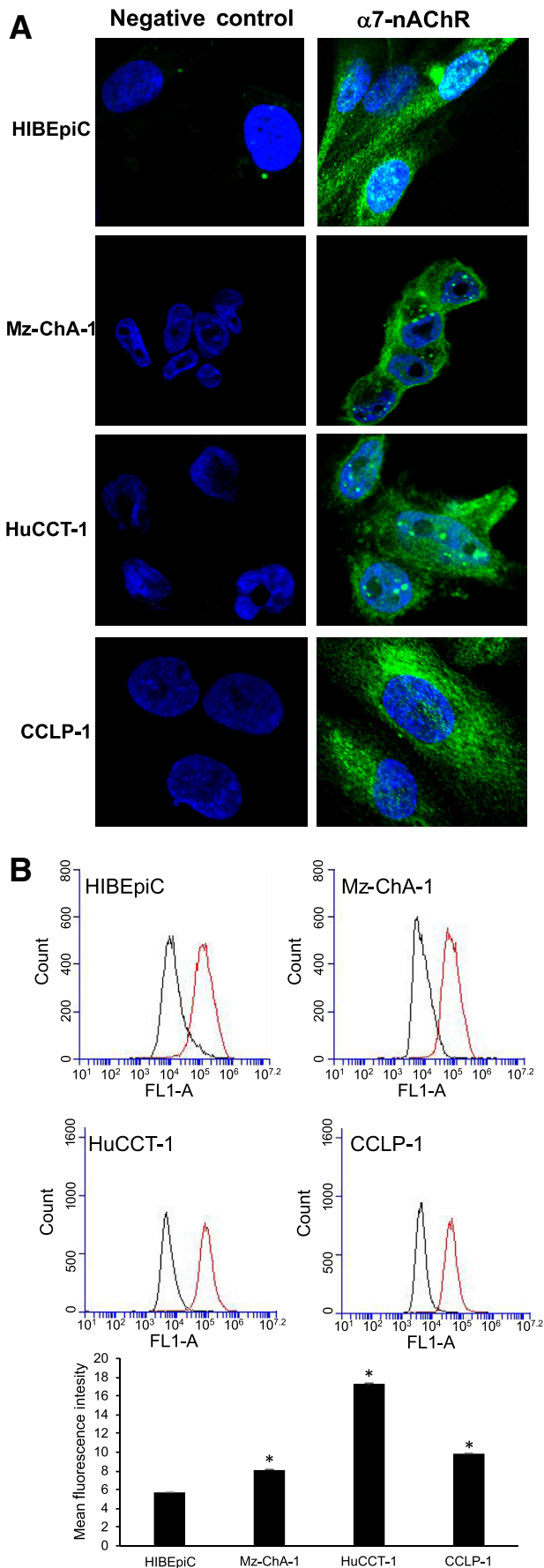
### Silencing of $\alpha 7$ -nAChR Expression in Mz-ChA-1 Cells

Mz-ChA-1 cells were transfected with a SureSilencing shRNA plasmid with a scrambled sequence (vector) that does not match any mammalian gene or  $\alpha 7$ -nAChR sequence (KR06841) (Qiagen, Duesseldorf, Germany). The plasmid contains a marker for G418 (Geneticin) resistance. Clones

**Table 1** Patient Characteristics

Characteristic	Healthy ( $n = 1$ )	CCA ( $n = 11$ )
Patients, $n$ (%)		
Male	1	4 (36.4)
Female		7 (63.6)
Age in years, means $\pm$ SEM		
Male	44	76.5 $\pm$ 3.5
Female		58.6 $\pm$ 4.1

CCA, cholangiocarcinoma.



were cultured in media that contained 5  $\mu\text{mol/L}$  of Geneticin for 2 weeks. Surviving clones were picked and seeded into plates and were maintained in media that contained 1  $\mu\text{mol/L}$  Geneticin. A total of four clones were evaluated by RT-PCR to verify the knockdown of the  $\alpha 7$ -nAChR gene. The RNeasy mini kit (Qiagen, Valencia, CA) was used to extract mRNA according to the manufacturer's instructions. The iScript cDNA Synthesis Kit (170-8891; Bio-Rad, Hercules, CA) was used for cDNA synthesis according to the manufacturer's instructions. RT-PCR was performed using the iTaq Universal SYBR Green Supermix (172-5121; Bio-Rad) according to the manufacturer's instructions. Human  $\alpha 7$ -nAChR-specific (PPH22901B) and glyceraldehyde-3-phosphate dehydrogenase-specific (PPH00150F) primers (Qiagen) were used. RT-PCR was performed with an ABI Prism 7900HT system using a two-step PCR program set at 95°C for 10 minutes, then 40 cycles of 95°C for 15 seconds, and 60°C for 1 minute. A  $\Delta\Delta C_T$  analysis was performed comparing the  $\alpha 7$ -nAChR knockdown clone to the vector-only control. The knockdown of  $\alpha 7$ -nAChR in Mz-ChA-1 cells treated with control and  $\alpha 7$ -nAChR shRNA was also evaluated by FACS for  $\alpha 7$ -nAChR expression as described earlier. The strongest knockdown (clone 3) was used in for the evaluation of proliferation by MTS assay and ERK 1/2 activity enzyme-linked immunosorbent assays (ELISAs).

#### Evaluation of the Effect of $\alpha 7$ -nAChR on Proliferation and p-ERK Activation in Mz-ChA-1 Cells

##### Immunofluorescence

Mz-ChA-1 cells were seeded at 10,000 cells per well into six-well plates that contained sterile coverslips and allowed to adhere overnight. Cells were treated with 10  $\mu\text{mol/L}$  nicotine and fixed at 0, 3, and 10 minutes after starting treatment. Immunofluorescence was performed as described above with the following exceptions: p-ERK 1/2 antibody (4370S; 1:200; Cell Signaling Technology, Danvers, MA) and Cy3 anti-rabbit secondary antibody (1:50; Jackson ImmunoResearch Laboratories) were used.

##### Western Blotting

Mz-ChA-1 cells were treated with 10  $\mu\text{mol/L}$  nicotine and 10  $\mu\text{mol/L}$  PNU282987 ( $\alpha 7$ -nAChR specific agonist; Tocris Bioscience, Bristol, UK)<sup>28</sup> in the presence or absence of 1 nmol/L  $\alpha 7$ -nAChR antagonist  $\alpha$ -bungarotoxin (Tocris Bioscience)<sup>28</sup> for 5 minutes and p-ERK 1/2 (Cell Signaling Technology), total ERK 1/2 (Cell Signaling Technology),

**Figure 1**  $\alpha 7$  nicotinic acetylcholine receptor ( $\alpha 7$ -nAChR) expression in normal human cholangiocytes and cholangiocarcinoma (CCA) cell lines. **A:** The expression of  $\alpha 7$ -nAChR in the normal human intrahepatic biliary epithelial cell (HIBEpiC) line and three human CCA cell lines, Mz-ChA-1, HuCCT-1, and CCLP-1, was verified by immunofluorescence. Green:  $\alpha 7$ -nAChR; blue: DAPI. **B:** The expression levels of  $\alpha 7$ -nAChR significantly increase in the human CCA lines compared with the HIBEpiC line evaluated by fluorescence-activated cell sorting. \* $P < 0.05$  versus HIBEpiC. Original magnification,  $\times 100$ .

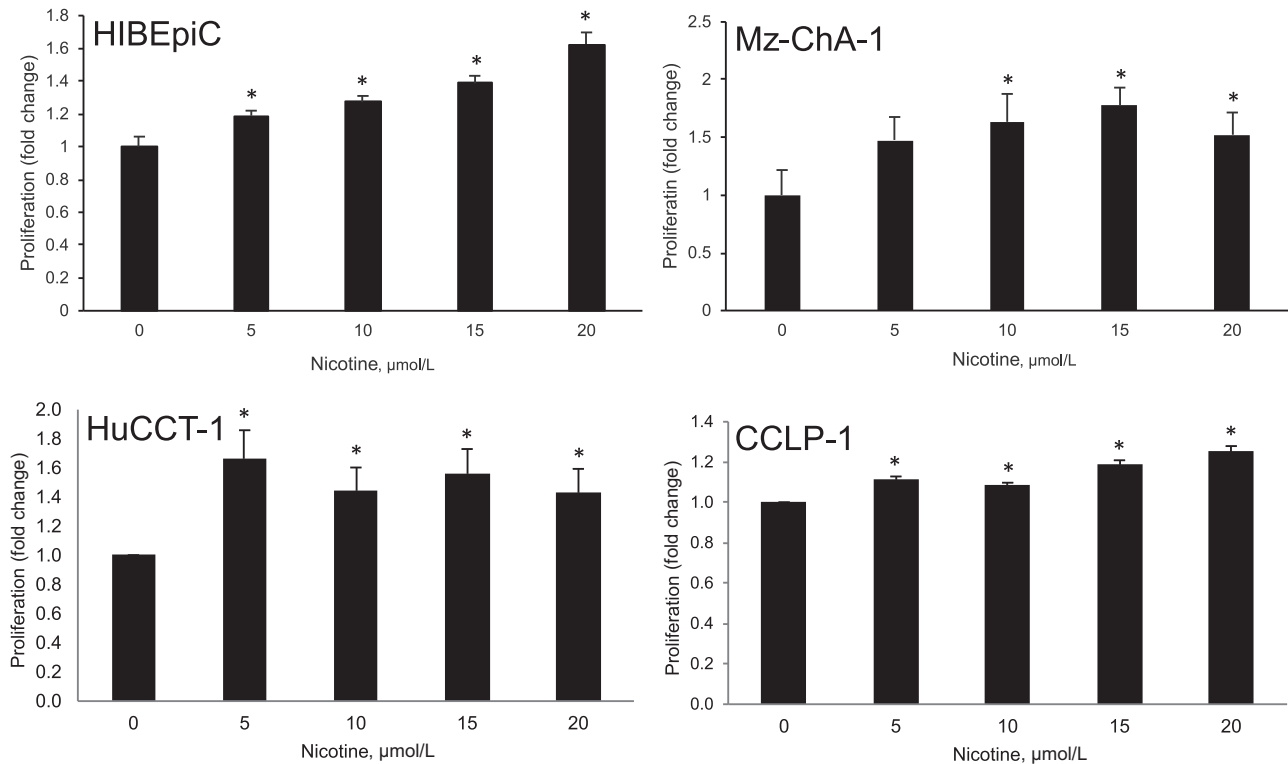


**Figure 2** Dose-dependent effects of nicotine on normal normal human intrahepatic biliary epithelial cell (HIBEpIC) and cholangiocarcinoma (CCA) cell line proliferation. Nicotine (0, 5, 10, 15, and 20  $\mu\text{mol/L}$ ) stimulates the proliferation of normal human cholangiocytes (HIBEpIC) and the three CCA cell lines at 48 hours of incubation evaluated by MTS proliferation assay. Data are expressed as means  $\pm$  SEM.  $n = 4$  experiments.  $*P < 0.05$  versus 0  $\mu\text{mol/L}$  nicotine.

and  $\beta$ -actin (loading control; Santa Cruz Biotechnology, Santa Cruz, CA) expression was evaluated by immunoblotting as previously described.<sup>29</sup>

#### MTS Proliferation Assay

Proliferation was evaluated as described earlier. Briefly, control shRNA- and  $\alpha 7$ -nAChR shRNA-transfected Mz-ChA-1 cell lines were incubated in the presence or absence of 10  $\mu\text{mol/L}$  nicotine for 48 hours.

#### ELISA

To evaluate the effect of  $\alpha 7$ -nAChR knockdown on p-ERK, cells were treated with 10  $\mu\text{mol/L}$  nicotine for 0, 2, 5, and 10 minutes. A cell-based ELISA for p-ERK and total ERK was performed on cell extracts according to the manufacturer's instructions (KCB1018) (R&D Systems, Minneapolis, MN).

#### In Vivo Experiments

##### Treatment Schedule

All animal experiments were performed according to protocols approved by the Baylor Scott & White Health Institutional Animal Care and Use Committee. Male BALB/c nude mice (Taconic Farms, Hudson, NY) were maintained in a temperature-controlled environment (20°C to 22°C) with a 12-hour light/dark cycle and with free access to standard mouse chow and drinking water. Mz-ChA-1 cells ( $5 \times 10^6$ ) suspended in 0.2 mL of extracellular matrix gel were injected s.c. into the

right and left rear flanks of the nude mice. Seven days after the injections, tumor establishment was verified by measuring the volume of each tumor (tumor volume was approximately 5  $\text{mm}^3$ ), and the mice were divided into the following groups: the first group ( $n = 6$ , control) received regular drinking water, the second group ( $n = 6$ , 50  $\mu\text{mol/L}$  nicotine) received drinking water that contained 50  $\mu\text{mol/L}$  nicotine, and the third group ( $n = 6$ , 200  $\mu\text{mol/L}$  nicotine) received drinking water with 200  $\mu\text{mol/L}$  nicotine. Previous studies have used this dosage range for studies in nude mice with xenografts.<sup>30–32</sup> The dose of nicotine used is within the range of daily nicotine intake in heavy smokers.<sup>33</sup> In a separate set of experiments, the mice were divided into two groups: the first group ( $n = 6$ , control) received 0.9% saline i.p. every other day, and the second group ( $n = 6$ , experimental) received 1 mg/kg of PNU282987 i.p.<sup>34</sup> every other day. Beginning with the first day of treatment, tumor volume was measured biweekly throughout the treatment period using an electronic caliper. Tumor volume was determined as follows: [tumor volume ( $\text{mm}^3$ ) =  $0.5 \times \text{length (mm)} \times \text{width (mm)} \times \text{height (mm)}$ ].

Thirty-eight days after beginning treatment, the mice were anesthetized with 50 mg/kg of sodium pentobarbital (i.p.) and sacrificed according to institutional guidelines. At this time, tumors were harvested and prepared for formalin fixation and paraffin embedding or lysed for protein or mRNA purification. For formalin-fixed, paraffin-embedded tumors, the tumors were fixed in 10% buffered formalin overnight before embedding in low-temperature paraffin and



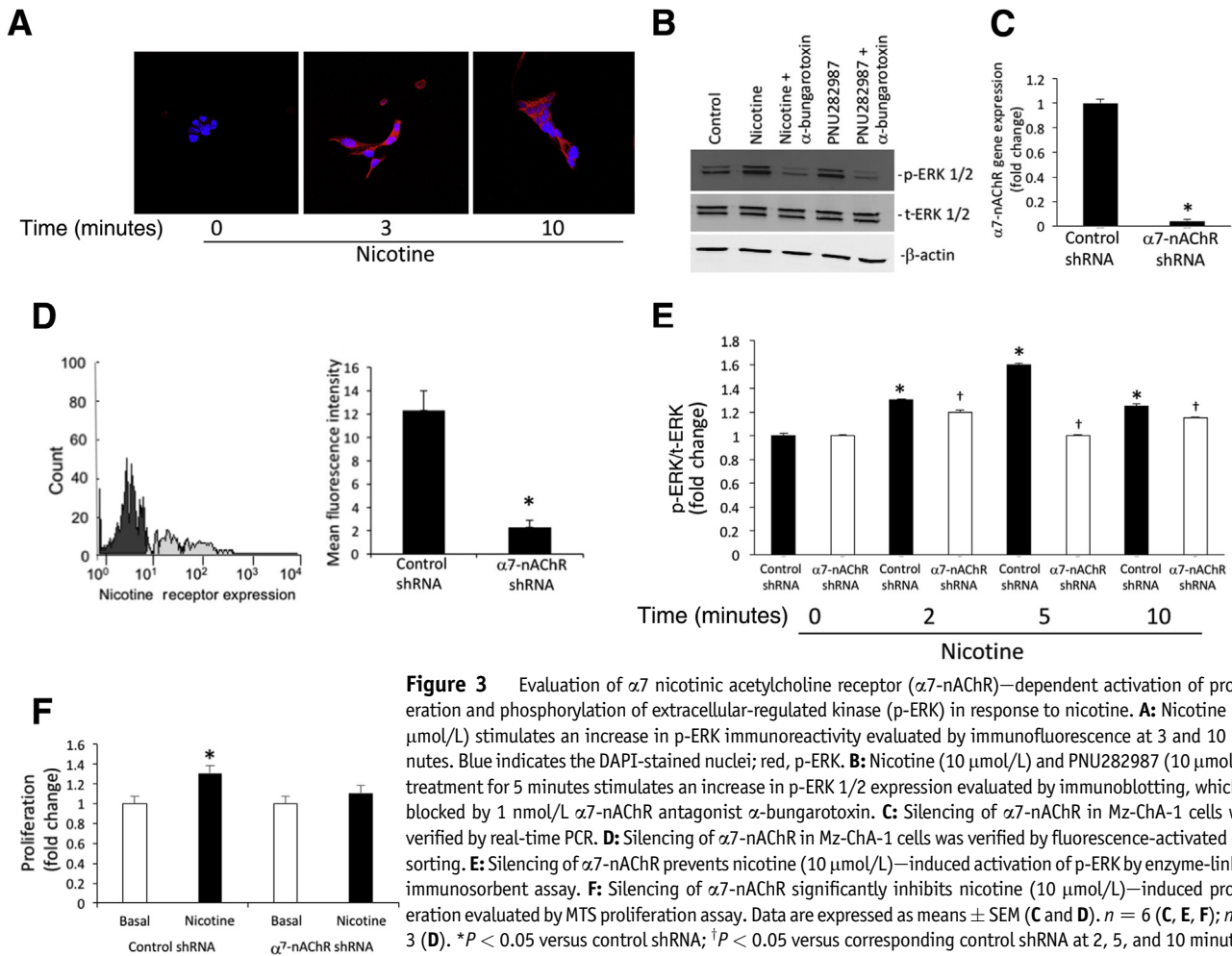


**Figure 3** Evaluation of  $\alpha 7$  nicotinic acetylcholine receptor ( $\alpha 7$ -nAChR)—dependent activation of proliferation and phosphorylation of extracellular-regulated kinase (p-ERK) in response to nicotine. **A:** Nicotine (10  $\mu\text{mol/L}$ ) stimulates an increase in p-ERK immunoreactivity evaluated by immunofluorescence at 3 and 10 minutes. Blue indicates the DAPI-stained nuclei; red, p-ERK. **B:** Nicotine (10  $\mu\text{mol/L}$ ) and PNU282987 (10  $\mu\text{mol/L}$ ) treatment for 5 minutes stimulates an increase in p-ERK 1/2 expression evaluated by immunoblotting, which is blocked by 1 nmol/L  $\alpha 7$ -nAChR antagonist  $\alpha$ -bungarotoxin. **C:** Silencing of  $\alpha 7$ -nAChR in Mz-ChA-1 cells was verified by real-time PCR. **D:** Silencing of  $\alpha 7$ -nAChR in Mz-ChA-1 cells was verified by fluorescence-activated cell sorting. **E:** Silencing of  $\alpha 7$ -nAChR prevents nicotine (10  $\mu\text{mol/L}$ )—induced activation of p-ERK by enzyme-linked immunosorbent assay. **F:** Silencing of  $\alpha 7$ -nAChR significantly inhibits nicotine (10  $\mu\text{mol/L}$ )—induced proliferation evaluated by MTS proliferation assay. Data are expressed as means  $\pm$  SEM (**C** and **D**).  $n = 6$  (**C**, **E**, **F**);  $n = 3$  (**D**). \* $P < 0.05$  versus control shRNA; † $P < 0.05$  versus corresponding control shRNA at 2, 5, and 10 minutes. Original magnification,  $\times 100$ . t-ERK, total extracellular-regulated kinase.

processed for slide preparation. Tumor sections (4  $\mu\text{m}$  thick) were used for hematoxylin and eosin (H&E) staining, Sirius Red staining, and immunohistochemistry (IHC).

#### H&E Staining

Tumor structure was evaluated using the H&E stain. The slides were deparaffinized, rehydrated, and stained with Harris Hematoxylin Solution (Sigma-Aldrich, St. Louis, MO) for 1 minute and counterstained with Eosin Y Solution (Fisher Scientific, Kalamazoo, MI). H&E-stained tumor sections were evaluated for necrosis, surrounding inflammation, and fibrosis by a hepatopathologist masked to all mouse data (Baylor Scott & White Health, Temple, TX).

#### Sirius Red Staining

Tumors were stained with PicroSirius Red Stain to assess collagen accumulation. Slides were deparaffinized, rehydrated, stained with Weigert's Iron Hematoxylin Solution (Sigma-Aldrich) for 10 minutes, counterstained with PicroSirius Red Solution (1.3% picric acid; Sigma-Aldrich) (0.001% Direct Red 80; Sigma-Aldrich) for 1 hour, and rinsed in 0.5% acetic acid. Sirius Red staining in light microscopy images was

quantitated in a coded fashion using ImageJ version 1.51j (NIH, Bethesda, MD; <http://imagej.nih.gov/ij>).<sup>35</sup>

#### IHC in Xenograft Tumors

Tumors from each group of mice ( $n = 3$ ) were evaluated for the expression of CK-19,  $\alpha 7$ -nAChR, S100A4, Ki-67, and p-ERK by IHC. The heat-mediated antigen retrieval step was performed using an antigen unmasking solution (Vector Laboratories, Burlingame, CA) and a modified microwave protocol to heat the solution. Briefly, after deparaffinization and rehydration, the slides were placed into a glass Coplin jar that contained the antigen unmasking solution that was diluted according to the manufacturer's instructions. The Coplin jar was placed into a beaker that contained 500 mL of water and covered in plastic wrap and microwaved on full power for 2.5 minutes followed by 10 minutes at 20% power. The Coplin jar that contained the slides was then removed from the beaker and allowed to sit at room temperature for 20 minutes before the tissues were fixed. Vectastain ABC kits (rabbit: PK-4001; goat: PK-4005; Vector Laboratories) were used for blocking, secondary antibodies, and avidin/biotinylated enzyme complex. The

following primary antibodies and conditions were used: CK-19 (ab52625, 1:200 dilution, 2 hours of incubation at room temperature),  $\alpha 7$ -nAChR (ab10096, 1:100 dilution, 2 hours of incubation at room temperature), S100A4 (13018S, 1:1000 dilution, 2 hours of incubation at room temperature), Ki-67 (ab15580, 1:200 dilution, 1 hour of incubation at room temperature), p-ERK (4370S, 1:150 dilution, 19 hours of incubation at 4°C) (Abcam and Cell Signaling Technology). A peroxidase substrate kit (SK-4100; Vector Laboratories) was used for antigen labeling. After antigen labeling, tissue sections were counterstained with Harris Hematoxylin Solution (Sigma-Aldrich). Quantification of Ki-67 immunoreactivity was assessed in a coded fashion by counting the number of Ki-67–positive nuclei per tumor section image ( $n = 3$  tumors per group; six images per tumor). Quantification of S100A4 and p-ERK 1/2 immunoreactivity was assessed in a coded fashion per tumor section image ( $n = 3$  tumors per group; six images per tumor) using ImageJ software.<sup>35,36</sup>  $\alpha 7$ -nAChR, CK-19, and S100A4 expression levels were evaluated by real-time PCR as previously described.<sup>14</sup>

### Evaluation of $\alpha 7$ -nAChR Expression in Human CCA Tissues

#### Human Tissue Array

The expression of  $\alpha 7$ -nAChR was evaluated in commercially available tissue array (ab17820; Abcam, <http://www.abcam.com/cholangiocarcinomas-paired-with-normal-liver-tissues-in-triplicates-126-samples-11mm-set-1-ab178201.html>, last accessed December 29, 2016). The array is a CCA/paired normal tissue array that contains one normal adjacent normal liver tissue paired with two tumor tissue cores from each patient. IHC was performed as described earlier for the xenograft tumors. Semiquantitative analysis was performed in a blind fashion (J.G.), using the following variables: staining intensity was assessed on a scale of 1 to 4 (1, no staining; 4, intense staining) and the abundance of positively stained cells was given a score of 1 to 5 (1, no cells stained; 5, 100% stained). The staining index was then calculated by the staining intensity multiplied by the staining abundance that gave a range of 1 to 20.

#### Human CCA Samples

RNA isolated from 11 CCA samples and one normal human liver were obtained from Dr. P. Invernizzi (Humanitas Research Hospital, Rozzano, Italy) under a protocol approved by the Ethics Committee by the Humanitas Research Hospital; the protocol was reviewed by the US Department of Veterans Affairs Institutional Review Board and Research and Development Committee. The protocol was approved by the Texas A&M Health Science Center Institutional Review Board. The tumor samples are described in Table 1. From these samples, the mRNA expression of  $\alpha 7$ -nAChR (NM\_000746) and glyceraldehyde-3-phosphate dehydrogenase (NM\_002046) was evaluated by real-time PCR using human primers

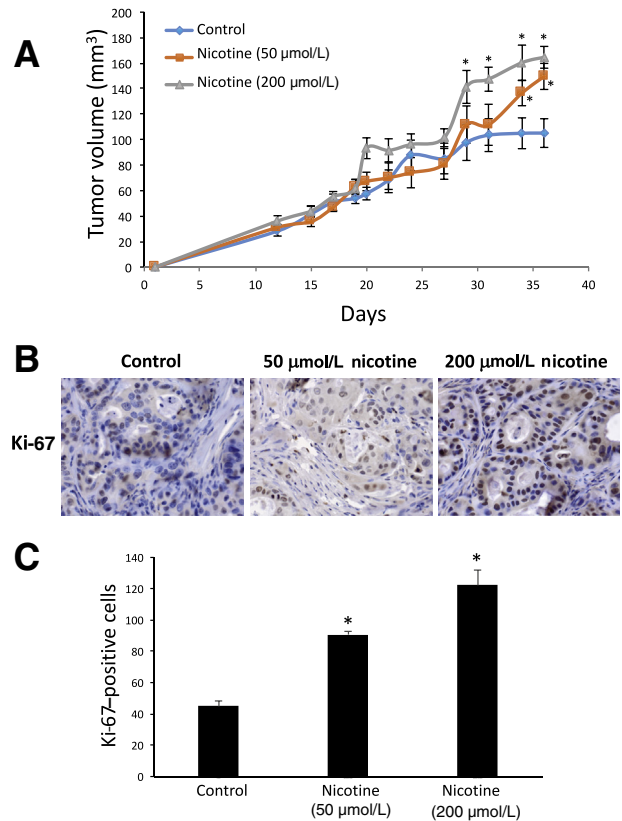


**Figure 4** Effect of nicotine administration on cholangiocarcinoma xenograft tumor volume and Ki-67 expression. **A:** Nicotine administration (50 and 200  $\mu\text{mol/L}$ ) stimulates a significant increase in tumor volume compared with control treatment. **B:** Nicotine administration (50 and 200  $\mu\text{mol/L}$ ) increases Ki-67 (cellular marker of proliferation) immunoreactivity in tumor sections compared with control treatment by immunohistochemistry. **C:** Nicotine administration (50 and 200  $\mu\text{mol/L}$ ) increases the number of Ki-67–positive cells. Data are expressed as means  $\pm$  SEM (**A** and **C**).  $n = 6$  mice per treatment group (2 tumors per mouse) (**A**);  $n = 3$  tumors (6 images of each tumor) (**C**). \* $P < 0.05$  versus control. Original magnification,  $\times 40$  (**B**).

purchased from Qiagen. The RNA was reverse transcribed using the Reaction Ready First Strand cDNA synthesis kit (Qiagen). SYBR Green PCR master mix (Qiagen) was used in the experimental assay. Real-time RT-PCR was performed with an ABI Prism 7900HT System using a two-step PCR cycling program at 95°C for 10 minutes followed by 40 cycles of 95°C for 15 seconds and 60°C for 1 minute. A  $\Delta\Delta C_T$  analysis was performed using normal human liver sample as the control.

### Statistical Analysis

All data are expressed as means  $\pm$  SEM. Differences between groups were analyzed by the unpaired  $t$ -test when two groups were analyzed and by the  $U$ -test and Kruskal-Wallis H test when more than two groups were analyzed, followed by an appropriate post hoc test.  $P < 0.05$  was considered significant.

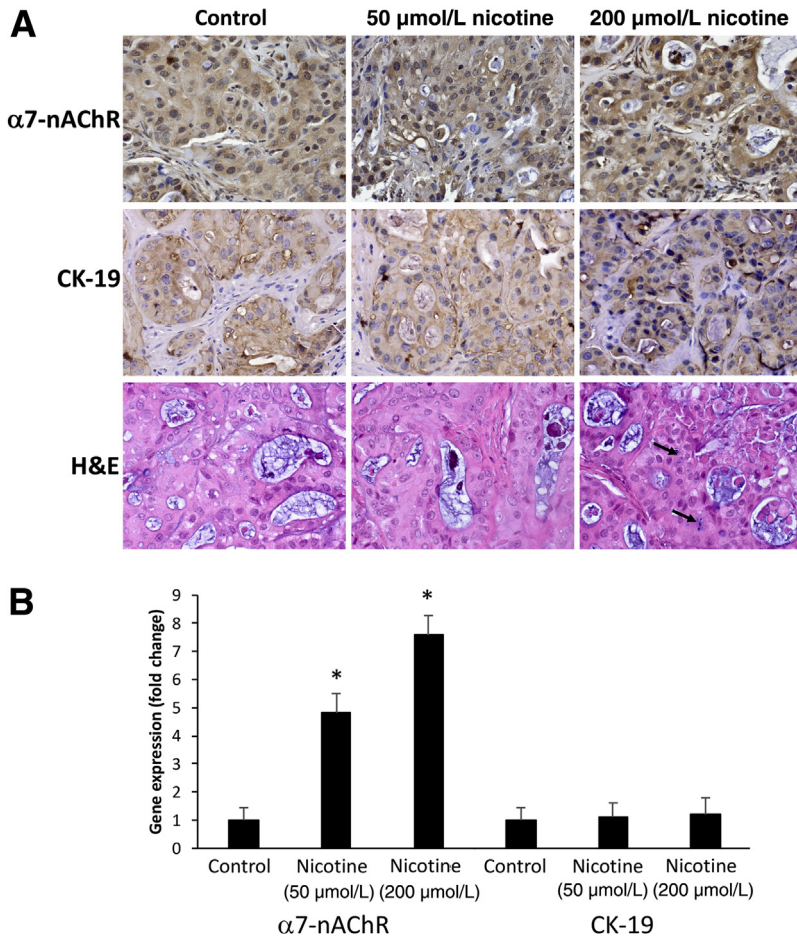


**Figure 5** Characterization of the cholangiocarcinoma (CCA) tumors from the xenograft mice. **A:** The expression of the  $\alpha 7$  nicotinic acetylcholine receptor ( $\alpha 7$ -nAChR) in the CCA tumors from the xenograft mice was verified by immunohistochemistry (IHC). CK-19 (cholangiocyte-specific marker) expression was verified by IHC. CCA tumor histologic features were evaluated by hematoxylin and eosin (H&E) staining. Inflammatory infiltrates are indicated by **arrows**. **B:**  $\alpha 7$ -nAChR expression levels evaluated by real-time PCR were found to be increased in xenograft tumors treated with nicotine (50 and 200  $\mu\text{mol/L}$ ) compared with control. CK-19 expression levels evaluated by real-time PCR were unchanged among the treatment groups. Data are expressed as means  $\pm$  SEM.  $n = 6$  (**B**). \* $P < 0.05$  versus control treatment. Original magnification,  $\times 40$ .

## Results

### $\alpha 7$ -nAChR Expression in Normal Human Cholangiocytes and CCA Cell Lines

$\alpha 7$ -nAChR was expressed in the normal human cholangiocyte cell line (HIBEpIC) and the three CCA cell lines (Mz-ChA-1, HuCCT-1, and CCLP-1) by immunofluorescence (Figure 1A).  $\alpha 7$ -nAChR expression was confirmed by FACS analysis, which revealed a significant increase in the  $\alpha 7$ -nAChR in Mz-ChA-1, HuCCT-1, and CCLP-1 compared with HIBEpIC (Figure 1B).

### Nicotine Stimulates Cell Proliferation and p-ERK Activation

To determine the effect of nicotine on cholangiocytes, proliferation was evaluated by MTS assay in normal human cholangiocytes and the CCA cell lines. Nicotine induced a significant increase in the proliferation of the HIBEpIC and CCA lines, Mz-ChA-1, HuCCT-1, and CCLP-1 at 48 hours (Figure 2). Since the ERK 1/2 signaling pathway has been implicated as the key pathway regulating proliferation of normal and CCA cells,<sup>14,37–39</sup> the effect of nicotine on

ERK 1/2 phosphorylation was explored. There was no significant p-ERK activation in Mz-ChA-1 cells before stimulation with nicotine (Figure 3A). p-ERK activation was increased 3 minutes after stimulation with nicotine and continued until 10 minutes after nicotine addition (Figure 3A).  $\alpha 7$ -nAChR-dependent p-ERK 1/2 was evaluated by Western blotting for p-ERK 1/2. There was an increase in p-ERK 1/2 in Mz-ChA-1 treated with nicotine and a specific agonist for  $\alpha 7$ -nAChR, PNU282987, which was blocked by a specific antagonist for  $\alpha 7$ -nAChR ( $\alpha$ -bungaratoxin) (Figure 3B). To verify that nicotine-induced proliferation and p-ERK activation was dependent on  $\alpha 7$ -nAChR, we used shRNA to knockdown the expression of  $\alpha 7$ -nAChR in Mz-ChA-1 cells. We verified that the expression of  $\alpha 7$ -nAChR was knocked down by RT-PCR and FACS (Figure 3, C and D). We found that there was a significant reduction in nicotine-induced proliferation in Mz-ChA-1 cells silenced for  $\alpha 7$ -nAChR (Figure 3E). As expected, there was no difference in p-ERK activation in the  $\alpha 7$ -negative cells compared with the vector control cells before nicotine addition. However, 2, 5, and 10 minutes after stimulation with nicotine, there was a significant decrease in p-ERK activation in  $\alpha 7$ -nAChR-transfected cells compared with vector control cells (Figure 3F).



## Effect of Nicotine on Tumor Proliferation *in Vivo*

The Mz-ChA-1 cell line was chosen for its ability to grow tumors in xenograft animals.<sup>40,41</sup> During the early time points of the experiment (from 0 to 20 days), all the treatment groups experienced a similar increase in tumor volume. By day 20 the tumors from the 200  $\mu\text{mol/L}$  nicotine treatment group began to increase in volume more quickly than the other treatment groups, and this trend continued throughout the treatment period (until day 38) (Figure 4A). Ki-67 IHC was used to assess proliferation in the tumor cells. Tumor sections from the nicotine-treated mice (50 and 200  $\mu\text{mol/L}$ ) had significantly more Ki-67-positive cells than the untreated control mice (Figure 4, B and C), which is consistent with increased tumor size.

## Characterization of CCA Xenograft Tumors $\alpha 7$ -nAChR and CK-19 Expression

$\alpha 7$ -nAChR was expressed at similar levels in the tumors from all three treatment groups (Figure 5). Tumors from all three treatment groups were found to be composed primarily of cholangiocytes based on CK-19 (cholangiocyte-specific marker) immunoreactivity (Figure 5A). The expression of  $\alpha 7$ -nAChR and CK-19 was also confirmed by real-time PCR. There was a significant increase in  $\alpha 7$ -nAChR expression in the nicotine-treated xenograft mice

(Figure 5B). CK-19 expression was unchanged among the treatment groups.

## CCA Xenograft Tumors Have Increased Fibrosis and S100A4 Expression

On the basis of histopathologic evaluation of H&E-stained tumor sections, we found more surrounding inflammation and fibrosis extending into the tumor in the tumors from the nicotine-treated animals compared with the untreated controls (Figure 5). Fibrosis in the tumors was then evaluated by PicroSirius Red staining to assess collagen accumulation. There was a significant increase in collagen accumulation in the tumors from the nicotine-treated animals compared with the untreated controls (Figure 6, A and C). S100A4 has recently been found to be elevated in CCA tissues and may be a prognostic marker for CCA.<sup>42–44</sup> There was a significant increase in S100A4-positive staining in the tumors from the nicotine-treated animals compared with the untreated controls (Figure 6, B and D).

## CCA Xenograft Tumors Have Increased p-ERK 1/2 Activation

The effect of nicotine on p-ERK 1/2 activation in the tumor sections was assessed by p-ERK 1/2 IHC. There was an increase in p-ERK 1/2-positive staining in the tumors from

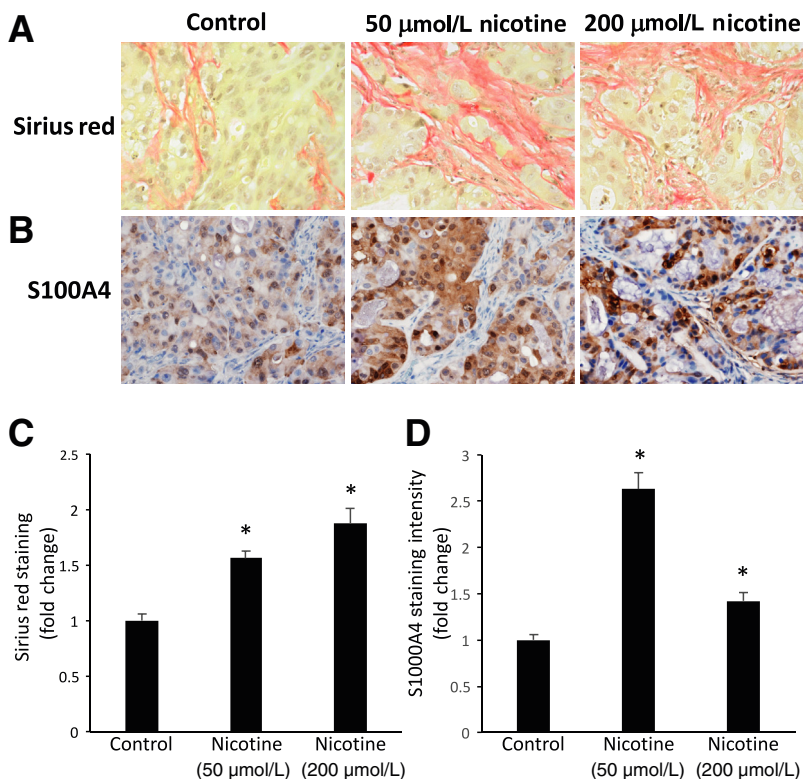


**Figure 6** Effect of nicotine administration of tumor fibrosis and S100A4 expression in cholangiocarcinoma (CCA) tumors from nicotine-treated xenograft mice. **A** and **C**: Nicotine administration (50 and 200  $\mu\text{mol/L}$ ) significantly increases fibrosis in the CCA tumors from xenograft mice evaluated by PicroSirius Red staining. **B** and **D**: Nicotine administration (50 and 200  $\mu\text{mol/L}$ ) stimulates the expression of the epithelial-mesenchymal transition marker (EMT), S100A4, in the CCA tumors from xenograft mice evaluated by immunohistochemistry. Data are expressed as means  $\pm$  SEM (**C** and **D**).  $n = 3$  tumors (6 images of each tumor) (**C** and **D**). \* $P < 0.05$  versus control treatment. Original magnification,  $\times 40$  (**A** and **B**).



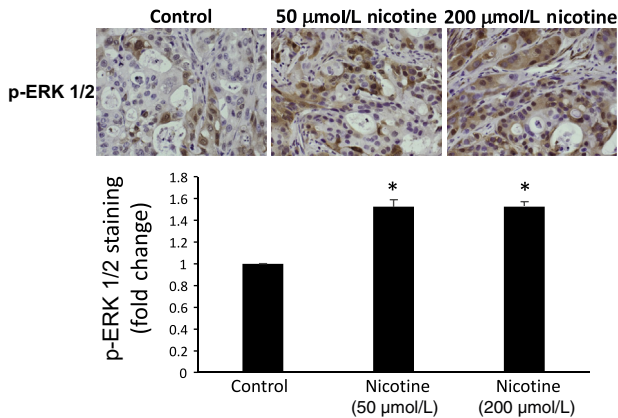


**Figure 7** Effect of nicotine administration on phosphorylation of extracellular-regulated kinase 1/2 (p-ERK  $1/2$ ) expression levels in cholangiocarcinoma tumors from nicotine-treated xenograft mice. Nicotine stimulates a significant increase in p-ERK  $1/2$  immunoreactivity. Data are expressed as means  $\pm$  SEM.  $n = 3$  tumors (6 images of each tumor). \* $P < 0.05$  versus control treatment. Original magnification,  $\times 40$ .

the nicotine-treated animals compared with the untreated controls (Figure 7).

### PNU282987, $\alpha 7$ -nAChR Agonist, Increases CCA Xenograft Tumor Growth, Fibrosis, and p-ERK $1/2$ Expression

During the early time points of the experiment (from 0 to 20 days), the treatment groups experienced a similar

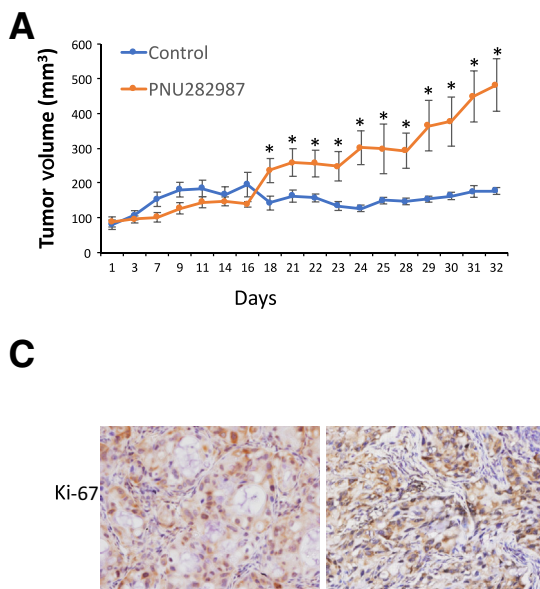
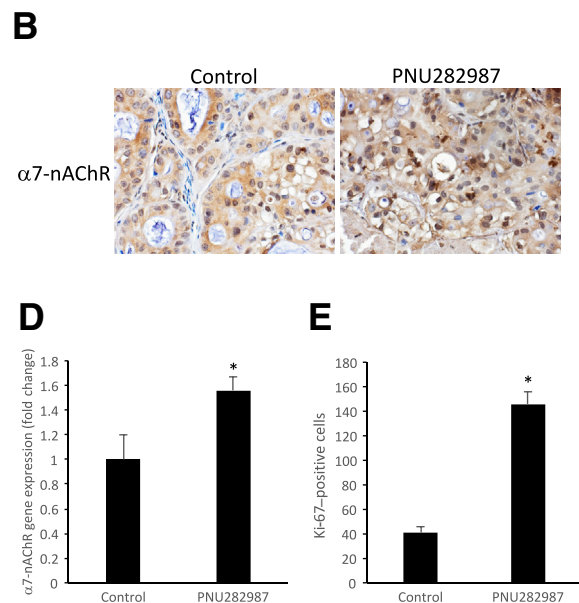


**Figure 8** Effect of PNU282987 administration on cholangiocarcinoma (CCA) xenograft tumor volume and  $\alpha 7$  nicotinic acetylcholine receptor ( $\alpha 7$ -nAChR) and Ki-67 expression. **A:** PNU282987 administration stimulates a significant increase in tumor volume compared with control treatment. **B:** The expression of  $\alpha 7$ -nAChR in the CCA tumors from the xenograft mice was verified by immunohistochemistry. **C:** PNU282987 administration increases Ki-67 (cellular marker of proliferation) immunoreactivity in tumor sections compared with control treatment by immunohistochemistry. **D:**  $\alpha 7$ -nAChR expression levels evaluated by real-time PCR were increased in xenograft tumors treated with PNU282987 compared with control. **E:** PNU282987 administration increases the number of Ki-67 positive cells. Data are expressed as means  $\pm$  SEM.  $n = 6$  mice per treatment group (2 tumors per mouse) (A);  $n = 3$  tumors (6 images of each tumor) (D and E). \* $P < 0.05$  versus control. Original magnification,  $\times 40$  (B and C).

increase in tumor volume. By day 18 the tumors from the PNU282987 treatment group began to increase in volume more quickly than the control treatment group, and this trend continued throughout the treatment period (until day 32) (Figure 8A).  $\alpha 7$ -nAChR expression was evaluated by IHC and real-time PCR (Figure 8, B and D). There was a significant increase in  $\alpha 7$ -nAChR expression in the PNU282987-treated xenograft tumors compared with control (Figure 8D). Ki-67 IHC was used to assess proliferation in the tumor cells. Tumor sections from the PNU282987-treated mice had significantly more Ki-67-positive cells than the untreated control mice (Figure 8, C and E), which is consistent with increased tumor size. There was a significant increase in collagen accumulation in the tumors from the PNU282987-treated animals compared with the controls (Figure 9, A and C). There was an increase in p-ERK  $1/2$ -positive staining in the tumors from the PNU282987-treated animals compared with the untreated controls (Figure 9, B and D). Finally, there was an increase in the S100A4 expression in the PNU282987-treated xenograft tumors (Figure 9E).

### Expression of $\alpha 7$ -nAChR in Human CCA Tumors

Finally, the expression of  $\alpha 7$ -nAChR in human CCA tumors was assessed by IHC.  $\alpha 7$ -nAChR expression was found to be significantly elevated in human CCA samples compared with nonmalignant paired liver samples (Figure 10A). The expression levels did not vary by grade. Lastly, we



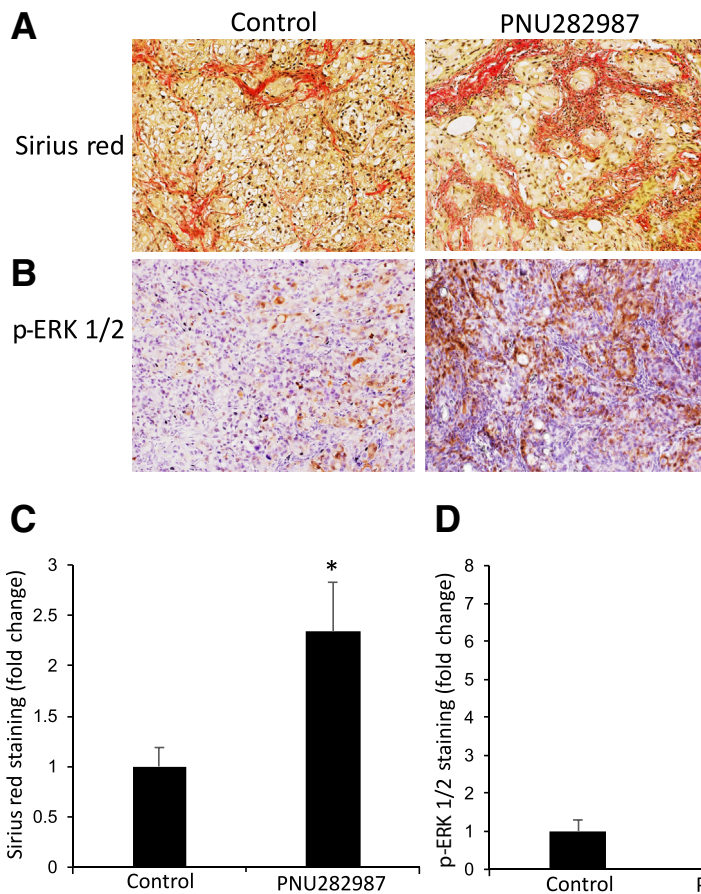


**Figure 9** Effect of PNU282987 administration on tumor fibrosis and phosphorylation of extracellular-regulated kinase 1/2 (p-ERK 1/2) and S100A4 expression in cholangiocarcinoma (CCA) tumors from xenograft mice. **A** and **C**: PNU282987 administration significantly increases fibrosis in the CCA tumors from xenograft mice evaluated by PicroSirius Red staining. **B** and **D**: PNU282987 administration stimulates a significant increase in p-ERK 1/2 immunoreactivity. **E**: PNU282987 administration stimulates the expression of the epithelial-mesenchymal transition marker, S100A4, in the CCA tumors from xenograft mice evaluated by real-time PCR. Data are expressed as means  $\pm$  SEM.  $n = 3$  tumors (6 images of each tumor). \* $P < 0.05$  versus control treatment. Original magnification,  $\times 40$  (**A** and **B**).

evaluated the expression of  $\alpha 7$ -nAChR in normal and human CCA tumor samples by real-time PCR. There was a significant increase in  $\alpha 7$ -nAChR mRNA levels in tumors from all three CCA grades compared with the normal control (Figure 10B).

## Discussion

Although there is conflicting evidence as to whether tobacco plays a role in the development and/or progression of CCA, the involvement of nicotine in this process likely represents a more complicated scenario involving comorbid conditions, such as PBC, PSC, and alcoholism. Research suggests that the past or current use of nicotine is a risk factor in the progression of cholestatic liver diseases.<sup>5–8,45–47</sup> In addition, long-term nicotine use in patients with PSC is a risk factor for the development of hepatobiliary cancers, including CCA.<sup>5–8,45–47</sup> Taken together, the results of these studies suggest that smoking may worsen pathologic liver conditions and predispose patients to malignant transformation. We previously found that nicotine has direct physiologic consequences on biliary epithelia, including intracellular signaling, proliferation, and production of profibrogenic components.<sup>14</sup> In this study, we further explored the effects of nicotine on CCA cells both *in vitro*

and *in vivo* in a mouse xenograft model. We also evaluated the expression of  $\alpha 7$ -nAChR in human CCA samples.

Here, we found that CCA cell lines express higher levels of  $\alpha 7$ -nAChR compared with the normal human cholangiocyte cell line HIBEpiC. The pentameric form of  $\alpha 7$ -nAChR is known to play a role in cell proliferation and pathogenesis in several diseases.<sup>15</sup> Nicotine stimulated the proliferation of CCA cell lines and the normal cholangiocyte line *in vitro* in a dose-dependent manner, which was partially blocked by silencing of  $\alpha 7$ -nAChR. Moreover, we found that nicotine and a specific  $\alpha 7$ -nAChR agonist (PNU282987) increases p-ERK 1/2 activation, which was partially blocked by  $\alpha 7$ -nAChR silencing. These results suggest that nicotine acts through  $\alpha 7$ -nAChR to stimulate the proliferation and the p-ERK 1/2 signaling pathway, which is known to stimulate cholangiocyte proliferation, hyperplasia, and malignancy.<sup>48–50</sup> Therefore, it is possible that nicotine acts as a mitogenic factor in pathogenesis of PBC and PSC to potentiate malignant transformation.

In the *in vivo* studies, we examined the morphologic features of cholangiocyte xenograft tumors, including cellular composition, inflammation, fibrosis, and S100A4 expression. First, we verified that the xenograft tumors were mostly composed of cholangiocytes by IHC for CK-19, a cholangiocyte-specific marker. Second, H&E-stained tumor sections were evaluated for the extent of

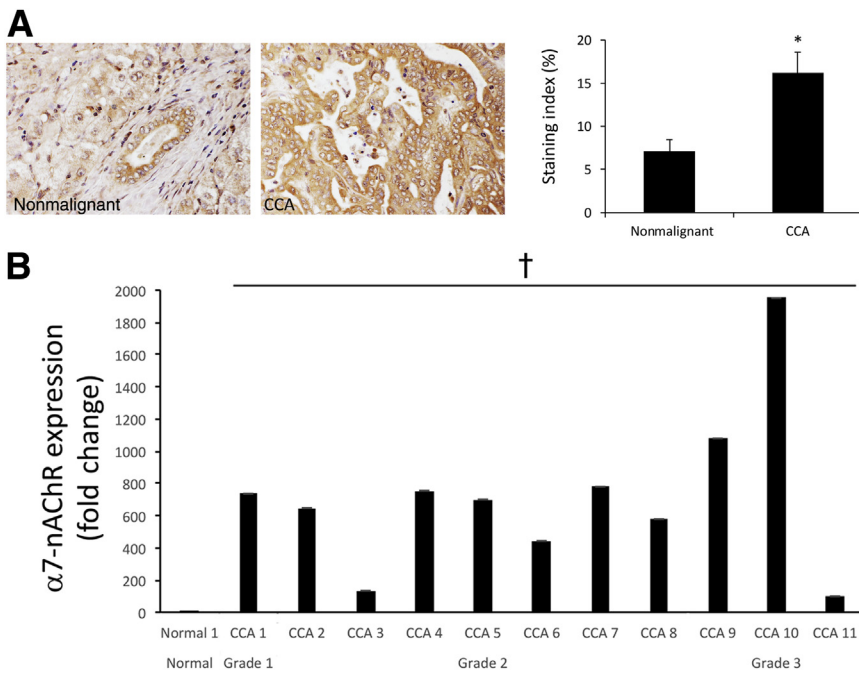


**Figure 10** Evaluation of  $\alpha 7$  nicotinic acetylcholine receptor ( $\alpha 7$ -nAChR) in human cholangiocarcinoma (CCA) samples. **A:**  $\alpha 7$ -nAChR immunoreactivity significantly increases in human CCA samples compared with nonmalignant controls in a commercially available tissue array. There is a significant increase in the staining index in human CCA samples compared with nonmalignant controls. **B:**  $\alpha 7$ -nAChR expression levels are significantly elevated in 11 human CCA samples by real-time PCR. Data are expressed as means  $\pm$  SEM (**A** and **B**).  $n = 42$  paired cases (**A**);  $n = 4$  for each sample (**B**). \* $P < 0.05$  versus nonmalignant control; † $P < 0.05$  versus normal human control liver sample. Original magnification,  $\times 40$ .

surrounding inflammation and fibrosis. Both surrounding inflammation and fibrosis extending into the tumor increased with increasing nicotine concentration. The extent of fibrosis was further evaluated by PicroSirius Red staining. Collagen deposition increased in the CCA tumors of the nicotine-treated xenograft mice compared with the untreated controls. We previously observed that nicotine stimulates fibrosis in the livers of normal rats, and it is well known that fibrosis is one of the consequences of chronic inflammation associated with many liver diseases, including PBC, PSC, and alcoholic liver disease.<sup>14</sup> The expression levels of S100A4 were also evaluated in the xenograft tumors, and there was a significant increase in S100A4 expression levels in the nicotine-treated xenograft mice compared with the untreated controls. Recent studies have found that S100A4 is elevated in CCA tissues and may be a prognostic marker for CCA.<sup>42–44</sup> Maternal nicotine exposure induces lung injuries and fibrosis in rat offspring, which was associated with increased S100A4.<sup>51</sup> The increase of S100A4 in the tumors of nicotine-treated xenograft mice suggests that nicotine exposure may stimulate the progression of CCA.

In addition to tumor morphologic features, nicotine stimulated the growth of CCA in our xenograft model. In addition, there was a significant nicotine-dependent increase in proliferation of the tumor cells, which is consistent with our *in vitro* observations. As expected,  $\alpha 7$ -nAChR is expressed in the CCA tumors in our xenograft mice from all treatment groups. The increase in proliferation observed in the CCA tumors of the nicotine-treated xenograft mice is likely due to the nicotine-dependent activation of  $\alpha 7$ -nAChR. Therefore, because we observed that the nicotine-dependent activation of

p-ERK in Mz-ChA-1 cells was dependent on  $\alpha 7$ -nAChR, we examined the activation of p-ERK in the CCA tumors by IHC. Consistent with the *in vitro* results, there was a dose-dependent increase in p-ERK activation in the CCA tumors of the nicotine-treated xenograft mice. To confirm the role of the  $\alpha 7$ -nAChR in nicotine-induced xenograft tumor growth and p-ERK 1/2, mice with xenograft tumors were treated with a specific agonist for  $\alpha 7$ -nAChR receptor, PNU282987. PNU282987 stimulated tumor growth and the p-ERK expression levels. These findings indicate that the activation of  $\alpha 7$ -nAChR plays an important role in the regulation of tumor growth and the downstream activation of ERK 1/2, which has been found to play a role in CCA growth in other studies.<sup>52</sup>

Finally, we verified that  $\alpha 7$ -nAChR is expressed in normal human liver tissue and CCA tissue and significantly elevated in CCA samples. Therefore, it is a reasonable assumption that nicotine-dependent activation of  $\alpha 7$ -nAChR in humans may promote the development and/or progression of CCA. However, the exact role of nicotine in this process, and specifically the signaling pathways involved, remains to be explored.

In summary, the results of this study indicate that nicotine stimulates CCA proliferation *in vitro*, which is likely the result of the  $\alpha 7$ -nAChR-dependent activation of p-ERK. In addition, nicotine accelerated the growth of the CCA tumors in our *in vivo* xenograft model and increased fibrosis, proliferation of the tumor cells, and p-ERK activation. Together, these findings suggest that nicotine participates in cholangiocarcinogenesis. In conclusion, our findings outline a novel role for nicotine in the progression of CCA growth and that nicotine use should be carefully considered when dealing with patients at risk for developing CCA.



## Acknowledgments

We thank Anna Web for her assistance with confocal imaging; and Drs. J. Gregory Fitz (UT Southwestern, Dallas, TX) and Anthony J. Demetris, (University of Pittsburgh, Pittsburgh, PA) for generously providing the Mz-ChA-1 and HuCC-T1 and CCLP1 cell lines, respectively.

## References

- World Health Organization, Research for International Tobacco Control: WHO Report on the Global Tobacco Epidemic, 2011: Warning about the Dangers of Tobacco. Geneva, Switzerland: World Health Organization, 2011
- Rivenson A, Hoffmann D, Prokopczyk B, Amin S, Hecht SS: Induction of lung and exocrine pancreas tumors in F344 rats by tobacco-specific and Aroclor-derived N-nitrosamines. *Cancer Res* 1988, 48:6912–6917
- Novello AC: Surgeon General's report on the health benefits of smoking cessation. *Public Health Rep* 1990, 105:545–548
- Vial M, Grande L, Pera M: Epidemiology of adenocarcinoma of the esophagus, gastric cardia, and upper gastric third. *Recent Results Cancer Res* 2010, 182:1–17
- Grainge MJ, West J, Soleymani-Dodaran M, Aithal GP, Card TR: The antecedents of biliary cancer: a primary care case-control study in the United Kingdom. *Br J Cancer* 2009, 100:178–180
- Shaib YH, El-Serag HB, Davila JA, Morgan R, McGlynn KA: Risk factors of intrahepatic cholangiocarcinoma in the United States: a case-control study. *Gastroenterology* 2005, 128:620–626
- Tyson GL, El-Serag HB: Risk factors for cholangiocarcinoma. *Hepatology* 2011, 54:173–184
- Welzel TM, Graubard BI, El-Serag HB, Shaib YH, Hsing AW, Davila JA, McGlynn KA: Risk factors for intrahepatic and extrahepatic cholangiocarcinoma in the United States: a population-based case-control study. *Clin Gastroenterol Hepatol* 2007, 5: 1221–1228
- Zhou YM, Yin ZF, Yang JM, Li B, Shao WY, Xu F, Wang YL, Li DQ: Risk factors for intrahepatic cholangiocarcinoma: a case-control study in China. *World J Gastroenterol* 2008, 14:632–635
- Cardenas L, Tremblay LK, Naranjo CA, Herrmann N, Zack M, Busto UE: Brain reward system activity in major depression and comorbid nicotine dependence. *J Pharmacol Exp Ther* 2002, 302:1265–1271
- Cahill K, Stead LF, Lancaster T: Nicotine receptor partial agonists for smoking cessation. *Cochrane Database Syst Rev* 2011:CD006103
- Hukkanen J, Jacob P 3rd, Benowitz NL: Metabolism and disposition kinetics of nicotine. *Pharmacol Rev* 2005, 57:79–115
- Benowitz NL: Drug therapy: pharmacologic aspects of cigarette smoking and nicotine addiction. *N Engl J Med* 1988, 319:1318–1330
- Jensen K, Afroze S, Ueno Y, Rahal K, Frenzel A, Sterling M, Guerrier M, Nizamutdinov D, Dostal DE, Meng F, Glaser SS: Chronic nicotine exposure stimulates biliary growth and fibrosis in normal rats. *Dig Liver Dis* 2013, 45:754–761
- Egleton RD, Brown KC, Dasgupta P: Nicotinic acetylcholine receptors in cancer: multiple roles in proliferation and inhibition of apoptosis. *Trends Pharmacol Sci* 2008, 29:151–158
- Schuller HM: Is cancer triggered by altered signalling of nicotinic acetylcholine receptors? *Nat Rev Cancer* 2009, 9:195–205
- Lazaridis KN, Gores GJ: Cholangiocarcinoma. *Gastroenterology* 2005, 128:1655–1667
- Marsh Rde W, Alonzo M, Bajaj S, Baker M, Elton E, Farrell TA, Gore RM, Hall C, Nowak J, Roy H, Shaikh A, Talamonti MS: Comprehensive review of the diagnosis and treatment of biliary tract cancer 2012. Part I: diagnosis-clinical staging and pathology. *J Surg Oncol* 2012, 106:332–338
- Alpini G, McGill JM, LaRusso NF: *The Pathobiology of Biliary Epithelia*. ed 4. Philadelphia, PA: Lippincott Williams & Wilkins, 2001
- Sirica AE: Cholangiocarcinoma: molecular targeting strategies for chemoprevention and therapy. *Hepatology* 2005, 41:5–15
- Knuth A, Gabbert H, Dippold W, Klein O, Sachsse W, Bitter-Suermann D, Prellwitz W, Meyer zum Buschenfelde KH: Biliary adenocarcinoma: characterisation of three new human tumor cell lines. *J Hepatol* 1985, 1:579–596
- Shimizu Y, Demetris AJ, Gollin SM, Storto PD, Bedford HM, Altarac S, Iwatsuki S, Herberman RB, Whiteside TL: Two new human cholangiocarcinoma cell lines and their cytogenetics and responses to growth factors, hormones, cytokines or immunologic effector cells. *Int J Cancer* 1992, 52:252–260
- Wu T, Leng J, Han C, Demetris AJ: The cyclooxygenase-2 inhibitor celecoxib blocks phosphorylation of Akt and induces apoptosis in human cholangiocarcinoma cells. *Mol Cancer Ther* 2004, 3:299–307
- Khalil AA, Jameson MJ, Broaddus WC, Lin PS, Chung TD: Nicotine enhances proliferation, migration, and radioresistance of human malignant glioma cells through EGFR activation. *Brain Tumor Pathol* 2013, 30:73–83
- Rezonzew G, Chumley P, Feng W, Hua P, Siegal GP, Jaimes EA: Nicotine exposure and the progression of chronic kidney disease: role of the alpha7-nicotinic acetylcholine receptor. *Am J Physiol Renal Physiol* 2012, 303:F304–F312
- Li H, Wang S, Takayama K, Harada T, Okamoto I, Iwama E, Fujii A, Ota K, Hidaka N, Kawano Y, Nakanishi Y: Nicotine induces resistance to erlotinib via cross-talk between alpha 1 nAChR and EGFR in the non-small cell lung cancer xenograft model. *Lung Cancer* 2015, 88:1–8
- Mosmann T: Rapid colorimetric assay for cellular growth and survival: application to proliferation and cytotoxicity assays. *J Immunol Methods* 1983, 65:55–63
- Lopez MG, Montiel C, Herrero CJ, Garcia-Palomo E, Mayorgas I, Hernandez-Guijo JM, Villarroya M, Olivares R, Gandia L, McIntosh JM, Olivera BM, Garcia AG: Unmasking the functions of the chromaffin cell alpha7 nicotinic receptor by using short pulses of acetylcholine and selective blockers. *Proc Natl Acad Sci U S A* 1998, 95:14184–14189
- Han Y, Onori P, Meng F, DeMorrow S, Venter J, Francis H, Franchitto A, Ray D, Kennedy L, Greene J, Renzi A, Mancinelli R, Gaudio E, Glaser S, Alpini G: Prolonged exposure of cholestatic rats to complete dark inhibits biliary hyperplasia and liver fibrosis. *Am J Physiol Gastrointest Liver Physiol* 2014, 307:G894–G904
- Al-Wadei HA, Plummer HK 3rd, Schuller HM: Nicotine stimulates pancreatic cancer xenografts by systemic increase in stress neurotransmitters and suppression of the inhibitory neurotransmitter gamma-aminobutyric acid. *Carcinogenesis* 2009, 30:506–511
- Wong HP, Yu L, Lam EK, Tai EK, Wu WK, Cho CH: Nicotine promotes colon tumor growth and angiogenesis through beta-adrenergic activation. *Toxicol Sci* 2007, 97:279–287
- Jarzyńska MJ, Guo P, Bar-Joseph I, Hu B, Cheng SY: Estradiol and nicotine exposure enhances A549 bronchioloalveolar carcinoma xenograft growth in mice through the stimulation of angiogenesis. *Int J Oncol* 2006, 28:337–344
- Lawson GM, Hurt RD, Dale LC, Offord KP, Croghan IT, Schroeder DR, Jiang NS: Application of serum nicotine and plasma cotinine concentrations to assessment of nicotine replacement in light, moderate, and heavy smokers undergoing transdermal therapy. *J Clin Pharmacol* 1998, 38:502–509
- Navarro E, Gonzalez-Lafuente L, Perez-Liebana I, Buendia I, Lopez-Bernardo E, Sanchez-Ramos C, Prieto I, Cuadrado A, Satrustegui J, Cadenas S, Monsalve M, Lopez MG: Heme-oxygenase I and PCG-1alpha regulate mitochondrial biogenesis via microglial activation of alpha7 nicotinic acetylcholine receptors using PNU282987. *Antioxid Redox Signal* 2016, [Epub ahead of print] doi:10.1089/ars.2016.6698



35. Schneider CA, Rasband WS, Eliceiri KW: NIH Image to ImageJ: 25 years of image analysis. *Nat Methods* 2012, 9:671–675
36. Schindelin J, Arganda-Carreras I, Frise E, Kaynig V, Longair M, Pietzsch T, Preibisch S, Rueden C, Saalfeld S, Schmid B, Tinevez JY, White DJ, Hartenstein V, Eliceiri K, Tomancak P, Cardona A: Fiji: an open-source platform for biological-image analysis. *Nat Methods* 2012, 9:676–682
37. Afroze SH, Munshi MK, Martinez AK, Uddin M, Gergely M, Szykarski C, Guerrier M, Nizamutdinov D, Dostal D, Glaser S: Activation of the renin-angiotensin system stimulates biliary hyperplasia during cholestasis induced by extrahepatic bile duct ligation. *Am J Physiol Gastrointest Liver Physiol* 2015, 308:G691–G701
38. Menakongka A, Suthiphongchai T: Involvement of PI3K and ERK1/2 pathways in hepatocyte growth factor-induced cholangiocarcinoma cell invasion. *World J Gastroenterol* 2010, 16:713–722
39. Alpini G, Kanno N, Phinizy JL, Glaser S, Francis H, Taffetani S, LeSage G: Tauroursodeoxycholate inhibits human cholangiocarcinoma growth via Ca<sup>2+</sup>-, PKC-, and MAPK-dependent pathways. *Am J Physiol Gastrointest Liver Physiol* 2004, 286:G973–G982
40. Onori P, Wise C, Gaudio E, Franchitto A, Francis H, Carpino G, Lee V, Lam I, Miller T, Dostal DE, Glaser SS: Secretin inhibits cholangiocarcinoma growth via dysregulation of the cAMP-dependent signaling mechanisms of secretin receptor. *Int J Cancer* 2010, 127:43–54
41. Meng F, DeMorrow S, Venter J, Frampton G, Han Y, Francis H, Standeford H, Avila S, McDaniel K, McMillin M, Afroze S, Guerrier M, Quezada M, Ray D, Kennedy L, Hargrove L, Glaser S, Alpini G: Overexpression of membrane metalloendopeptidase inhibits substance P stimulation of cholangiocarcinoma growth. *Am J Physiol Gastrointest Liver Physiol* 2014, 306:G759–G768
42. Tehasen A, Namwat N, Loilome W, Duangkumpha K, Puapairoj A, Saya H, Yongvanit P: Tumor necrosis factor-alpha modulates epithelial mesenchymal transition mediators ZEB2 and S100A4 to promote cholangiocarcinoma progression. *J Hepatobiliary Pancreat Sci* 2014, 21:703–711
43. Tian X, Wang Q, Li Y, Hu J, Wu L, Ding Q, Zhang C: The expression of S100A4 protein in human intrahepatic cholangiocarcinoma: clinicopathologic significance and prognostic value. *Pathol Oncol Res* 2015, 21:195–201
44. Ruys AT, Groot Koerkamp B, Wiggers JK, Klumpen HJ, ten Kate FJ, van Gulik TM: Prognostic biomarkers in patients with resected cholangiocarcinoma: a systematic review and meta-analysis. *Ann Surg Oncol* 2014, 21:487–500
45. Dam MK, Flensburg-Madsen T, Eliassen M, Becker U, Tolstrup JS: Smoking and risk of liver cirrhosis: a population-based cohort study. *Scand J Gastroenterol* 2013, 48:585–591
46. Corpechot C, Gaouar F, Chretien Y, Johanet C, Chazouilleres O, Poupon R: Smoking as an independent risk factor of liver fibrosis in primary biliary cirrhosis. *J Hepatol* 2012, 56:218–224
47. Bergquist A, Glaumann H, Persson B, Broome U: Risk factors and clinical presentation of hepatobiliary carcinoma in patients with primary sclerosing cholangitis: a case-control study. *Hepatology* 1998, 27:311–316
48. Banales JM, Masyuk TV, Gradilone SA, Masyuk AI, Medina JF, LaRusso NF: The cAMP effectors Epac and protein kinase A (PKA) are involved in the hepatic cystogenesis of an animal model of autosomal recessive polycystic kidney disease (ARPKD). *Hepatology* 2009, 49:160–174
49. Fava G, Marucci L, Glaser S, Francis H, De Morrow S, Benedetti A, Alvaro D, Venter J, Meininger C, Patel T, Taffetani S, Marzioni M, Summers R, Reichenbach R, Alpini G: Gamma-Aminobutyric acid inhibits cholangiocarcinoma growth by cyclic AMP-dependent regulation of the protein kinase A/extracellular signal-regulated kinase 1/2 pathway. *Cancer Res* 2005, 65:11437–11446
50. Glaser S, Lam IP, Franchitto A, Gaudio E, Onori P, Chow BK, Wise C, Kopriva S, Venter J, White M, Ueno Y, Dostal D, Carpino G, Mancinelli R, Butler W, Chiasson V, DeMorrow S, Francis H, Alpini G: Knockout of secretin receptor reduces large cholangiocyte hyperplasia in mice with extrahepatic cholestasis induced by bile duct ligation. *Hepatology* 2010, 52:204–214
51. Chen CM, Chou HC, Huang LT: Maternal nicotine exposure induces epithelial-mesenchymal transition in rat offspring lungs. *Neonatology* 2015, 108:179–187
52. Leelawat K, Keeratchamroen S, Leelawat S, Tohtong R: CD24 induces the invasion of cholangiocarcinoma cells by upregulating CXCR4 and increasing the phosphorylation of ERK1/2. *Oncol Lett* 2013, 6:1439–1446